Valproic acid causes dose- and time-dependent changes in nuclear structure in prostate cancer cells *in vitro* and *in vivo*

Madeleine S.Q. Kortenhorst,[1,3] Sumit Isharwal,[2] Paul J. van Diest,[3] Wasim H. Chowdhury,[2] Cameron Marlow,[2] Michael A. Carducci,[1] Ronald Rodriguez,[2] and Robert W. Veltri[2]

[1]Prostate Cancer Program, Sidney Kimmel Comprehensive Cancer Center at Johns Hopkins University; [2]James Buchanan Brady Urological Institute, Johns Hopkins University School of Medicine, Baltimore, Maryland and [3]Department of Pathology, University Medical Center Utrecht, Utrecht, The Netherlands

Abstract

Histone deacetylase inhibitors such as valproic acid (VPA) are promising anticancer agents that change the acetylation status of histones and loosen the chromatin structure. We assessed nuclear structure changes induced by VPA in prostate cancer LNCaP, CWR22R, DU145, and PC3 cell lines and xenografts and their potential use as a biomarker of treatment. *In vitro* tissue microarrays consisted of prostate cancer cell lines treated for 3, 7, or 14 days with 0, 0.6, or 1.2 mmol/L VPA. *In vivo* tissue microarrays consisted of cores from prostate cancer xenografts from nude mice treated for 30 days with 0.2% or 0.4% VPA in drinking water. Digital images of at least 200 Feulgen DNA-stained nuclei were captured using the Nikon CoolScope and nuclear alterations were measured. With a set of seven most frequently significant nuclear alterations (determined by univariate logistic regression analysis), control and VPA treatment nuclei were compared *in vitro* and *in vivo.* Depending on the cell line, area under the curve-receiver operating characteristics ranged between 0.6 and 0.9 and were dose- and time-dependent both *in vitro* and *in vivo*. Also, VPA treatment caused significant nuclear alterations in normal drug-filtering organs (liver and kidney tissue). *In vitro* and *in vivo* VPA treatment of prostate cancer cell lines results in significant dose- and time-dependent changes in nuclear structure. Further, VPA induces nuclear structural changes in normal liver and kidney tissue, which likely reflects a natural physiologic response. Therefore, nuclear structural alterations may serve as a biomarker for histone deacetylase inhibitor treatment. (Mol Cancer Ther 2009;8(4):802–8)

Introduction

Acetylation of histones and other nuclear proteins plays an important role in cancer development and progression (1). Deregulation of the balance between histone acetyltransferases and histone deacetylase (HDAC) has been associated with oncogenesis in many tissues (2, 3). HDAC inhibitors (HDACI) are promising anticancer agents that have shown stable disease and partial responses in a wide range of solid malignancies, including prostate cancer (4, 5). Recently, the Food and Drug Administration-approved HDACI vorinostat for the treatment of advanced cutaneous T-cell lymphoma. Clinical trials treating solid tumors with HDACI valproic acid (VPA) alone or combination are ongoing (6–8). Recently, two phase I clinical trials were published using VPA in combination with methyltransferase inhibitor 5-azacytidine or topoisomerase II inhibitor epirubicin (9, 10). These trials showed pharmacokinetic properties and toxicity profiles of VPA in patients with solid malignancies. In addition, stable disease and partial responses were reported in up to 39% and 22% of patients, respectively.

HDACIs change the acetylation status of histones, thereby enhancing the accessibility of the transcription and DNA repair machinery to DNA (11, 12). In addition to changing DNA accessibility by histone acetylation, HDACIs affect transcription, acetylation status, and function of proteins that are important for DNA mobility, DNA structure, and regulation of DNA accessibility (1, 13). Among these proteins are high-mobility group proteins (14–17), nuclear matrix proteins (18), tubulin (19, 20), and members of SWI/SNF complex (21).

Diamond and associates (22) were the first to employ nuclear structure measurements (nuclear roundness factor) by digital imaging to predict prostate cancer outcome. Subsequently, several investigators (23–28) have used nuclear alterations to predict pathologic stage and prognosis for prostate cancer patients. Nuclear morphometric alterations measured by computer-assisted image analysis can detect abnormal DNA content representing large-scale chromosomal alterations (tetraploidy and aneuploidy) reflecting genetic instability in tumor cells (29, 30). In addition, alterations in nuclear size, shape, and texture can be measured. In the current study, we assessed the nuclear structure changes induced by VPA treatment in prostate cancer cell lines

Received 12/22/08; accepted 1/9/09.

Grant support: Patana Fund, Prostate Cancer Foundation, Johns Hopkins University Prostate Cancer SPORE grant P50CA58236, Early Detection Research Network National Cancer Institute/NIH grant CA086323-06, Internationalization Grant University Medical Center Utrecht, and Aegon Foundation.

The costs of publication of this article were defrayed in part by the payment of page charges. This article must therefore be hereby marked *advertisement* in accordance with 18 U.S.C. Section 1734 solely to indicate this fact.

Note: M.S.Q. Kortenhorst and S. Isharwal contributed equally to this work.

Requests for reprints: Robert W. Veltri, James Buchanan Brady Urological Institute, Johns Hopkins University School of Medicine, 600 North Wolfe Street, Baltimore, MD 21287. Phone: 410-614-6380; Fax: 410-614-3695. E-mail: rveltri1@jhmi.edu

doi:10.1158/1535-7163.MCT-08-1076

and xenografts and their potential use as a biomarker of treatment.

Materials and Methods

Tissue Microarray

In vitro. The LNCaP, PC3, DU145, and C4-2 cell lines were grown in RPMI 1640 with L-glutamine (Cellgro) supplemented with 10% heat-inactivated fetal bovine serum (Life Technologies), 5 μg/mL ciprofloxacin hydrochloride (U.S. Biological), and 50 μg/mL gentamicin (Quality Biological). Cells were allowed to grow until 80% to 90% confluent and harvested with 0.05% trypsin/0.53 mmol/L EDTA (Cellgro) before each subsequent passage. VPA (1 mol/L; VPA sodium salt; Sigma) stock was made in PBS and filters were sterilized through a 0.22 μm filter. The *in vitro* tissue microarray consisted of core cell plugs from formalin-fixed, paraffin-embedded human prostate cancer cell lines LNCaP, C4-2, DU145, and PC3. Cells were treated for 3, 7, or 14 days with 0, 0.6, or 1.2 mmol/L VPA and resuspended in agarose before harvesting and paraffin embedding.

In vivo. Human prostate cancer cell lines LNCaP, PC3, DU145, and C4-2 were allowed to grow to 80% to 90% confluency and harvested as described above. Cells were resuspended in 1× PBS (pH 7.4; BioSource), mixed 1× with Matrigel (BD Biosciences), and injected (1×10^6 per injection) s.c. into the lateral flanks of male athymic *nu/nu* mice. Once palpable tumors were established, animals were randomized into control and treatment arms with the latter receiving 0.2% or 0.4% VPA in drinking water for 30 days before formalin fixation and paraffin embedding.

Tissue microarrays were prepared using a Beecher MT1 manual arrayer (Beecher Instruments). From formalin-fixed, paraffin-embedded tissue blocks, a spot was punched and transferred to a recipient block. The *in vitro* tissue microarray was constructed using two or three serial 0.60 mm core tissue samples from each cell plug. The *in vivo* tissue microarray was constructed using two serial 0.60 mm core tissue samples from each of the 4 to 10 replicate xenografts and 6 μm slides were prepared from each tissue microarray.

Digital Measurement of Nuclear Morphometric Alterations

Feulgen DNA staining was done per manufacturer's instructions (TriPath Imaging). Feulgen specifically and quantitatively stains DNA in cellular material by uncovering the free aldehyde groups in the DNA during the acid hydrolysis process, which then reacts with the Feulgen reagent to form a stable, blue color that absorbs light at 560 nm (31, 32). Figure 1 shows Feulgen-stained *in vitro* and *in vivo* tissue microarray spots.

Next, a minimum of 200 nuclei was captured from each tissue microarray spot using Nikon CoolScope imaging system with pathology software suite designed by Bacus Laboratories. The software calculates a total of 39 nuclear structure alterations using a single-step pixel analysis of

Figure 1. Feulgen-stained nuclei from prostate cancer cell line PC3. Untreated prostate cancer cells are smaller in diameter and more intensely stained than cells that have been either treated *in vitro* for 14 d with 1.2 mmol/L VPA (**A**) or *in vivo* for 30 d with 0.4% VPA in drinking water (**B**).

Table 1. Summary of *in vitro* samples used to study the effect of the HDACI VPA on nuclear morphometry of prostate cancer cell lines

	Day 3 (0 vs 0.6 mmol/L VPA)	Day 3 (0 vs 1.2 mmol/L VPA)	Day 7 (0 vs 0.6 mmol/L VPA)	Day 7 (0 vs 1.2 mmol/L VPA)	Day 14 (0 vs 0.6 mmol/L VPA)	Day 14 (0 vs 1.2 mmol/L VPA)
C4-2	367 (152/215)	277 (152/125)	413 (207/206)	344 (207/137)	773 (397/376)	732 (397/335)
DU145	365 (242/123)	420 (242/178)	**208 (208/0)**	339 (208/131)	808 (403/405)	761 (403/358)
LNCAP	417 (220/197)	397 (220/177)	214 (107/107)	337 (107/230)	746 (364/382)	699 (364/335)
PC3	**166 (112/54)**	**134 (112/22)**	**203 (119/84)**	**119 (119/0)**	532 (227/305)	600 (227/373)

NOTE: Those in bold were not considered for analyses; 166 (112 of 54) means 112 cells in control group and 54 cells in treated group.

each nucleus to quantitatively characterize nuclear size, shape, DNA content, and chromatin texture features. Tables 1 and 2 shows the number of nuclei captured from each treatment arm.

Statistical Analysis

All data were analyzed using Stata v10.0 statistical analysis software (Stata). Univariate logistic regression analysis was done to determine which independent variables significantly differentiate between VPA and control groups. Two sets of the most common univariately significant nuclear structure alterations, one for *in vitro* and one for *in vivo* experiments, were chosen to compare VPA response using area under the curve-receiver operating characteristic (AUC-ROC) across different doses and different durations for *in vitro* and *in vivo* experiments. Statistical significance in this study was set as $P \leq 0.05$.

Results

VPA Causes Dose- and Time-Dependent Changes in Prostate Cancer Nuclei *In vitro*

To assess nuclear structure changes induced by VPA treatment in LNCaP, C4-2, DU145, and PC3 cell lines, 39 features of nuclear size and shape, texture, and DNA content were measured using Nikon CoolScope imaging system (supplementary text contains definition of all features). Univariate logistic regression analysis with a variable selection stringency of $P_z \leq 0.05$ was done to identify significant alterations in nuclear structure after treatment with VPA for each cell line at each given dose and duration of treatment (Supplementary Table S1).[4] A set of the seven most frequently significant nuclear structural alterations was selected to compare VPA drug response across all prostate cancer cell lines tested at each given dose and duration of treatment. These included maximum diameter, peak, valley, difference entropy, information measure A, maximum correlation, and product moment. Figure 2 shows that alterations in nuclear structure were dose- and time-dependent and highest at 14 days of treatment with 1.2 mmol/L VPA. The increase in VPA response was minimal when 3 days of treatment was compared with 7 days of treatment. The PC3 nuclei showed the largest change in nuclear structure compared with LNCaP, C4-2, and DU145 at 14 days of treatment with 1.2 mmol/L VPA. We were unable to capture sufficient nuclear images at days 3 and 7 for the PC3 cell line with 0.6 and 1.2 mmol/L VPA and day 7 with 0.6 mmol/L VPA for DU145 cell line. These were therefore excluded from analysis.

In vivo Treatment with VPA Results in Nuclear Structure Changes

To determine whether the changes seen *in vitro* also occur *in vivo*, LNCaP, CWR22R, DU145, and PC3 xenografts were analyzed. Univariate logistic regression analysis with a variable selection stringency level of $P_z \leq 0.05$ was done to identify significant alterations in nuclear structure in xenografts after treatment of nude mice with VPA (Supplementary Table S2).[4] A set of the seven most frequently significant nuclear structural alterations were selected to compare VPA response across all xenograft experiments. These included maximum diameter, minimum diameter, average absorbance, SD, peak, valley, and triangular symmetry. Figure 3 shows that the quantitative changes in nuclear structure seen *in vivo* are dose-dependent. The extent of structural changes differed across different xenografts. The C4-2 xenograft tumors treated with 0.4% VPA treatment for 30 days showed the most pronounced change of all tested xenografts.

VPA Treatment Causes Nuclear Structural Changes in Normal Liver and Kidney

To assess whether VPA treatment also affects nuclear structure in drug-metabolizing and drug-filtering organs that appear normal by H&E staining, we captured images of normal liver and kidney cell nuclei 30 days after injection

Table 2. Summary of *in vivo* samples used to study the effect of the HDACI VPA on nuclear morphometry of prostate cancer cell lines and normal tissue

	Control vs 0.2% VPA	Control vs 0.4% VPA
PC3	1,119 (4) vs 701 (4)	1,119 (4) vs 1,260 (6)
DU145	NA	1,975 (10) vs 2,010 (9)
LNCaP	NA	823 (5) vs 1,147 (6)
C4-2	NA	1,463 (7) vs 1,424 (7)
CWR22R	1,323 (6) vs 863 (4)	1,323 (6) vs 695 (3)
Liver	NA	940 (4) vs 1,190 (5)
Kidney	NA	1,522 (6) vs 1,358 (5)

NOTE: 1,119 (4) vs 701 (4) means 1,119 cells captured from 4 xenografts for control and 701 cells captured from 4 xenografts for 0.2% VPA.

[4] Supplementary material for this article is available at Molecular Cancer Therapeutics Online (http://mct.aacrjournals.org/).

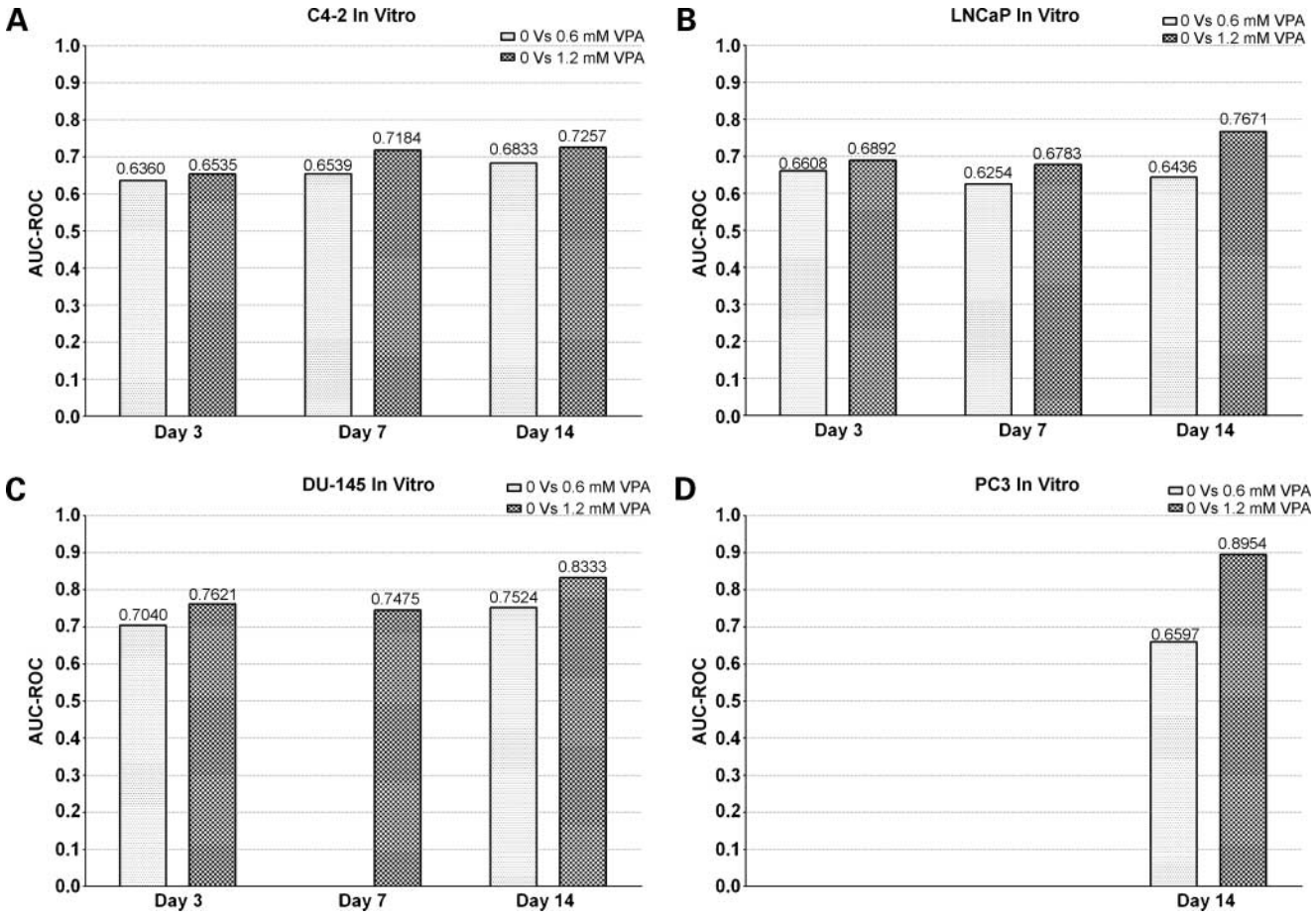

Figure 2. Summary of AUC-ROC statistics of control versus *in vitro* treated cell lines. **A** to **D,** response (AUC-ROC) of C4-2, LNCaP, DU145, and PC3 cell lines treated *in vitro* at different doses (0, 0.6, and 1.2 mmol/L VPA) and durations (3, 7, and 14 d) of VPA, respectively.

of tumor cells and compared them with mice injected and treated for 30 days with 0.4% VPA. Supplementary Table 2^4 shows significant nuclear alterations in liver and kidney after treatment. Using the abovementioned xenograft set of significant nuclear structure alterations (maximum diameter, minimum diameter, average absorbance, SD, peak, valley, and triangular symmetry), AUC-ROC for liver and kidney were 0.64 and 0.71, respectively.

Discussion

Malignant diseases are exemplified by aberrant transcriptional regulation that may be triggered by a change in recruitment of HDACs to the site of transcriptional initiation (33). Screening of HDAC expression in human prostate cancer has revealed distinct class I HDAC profiles between stromal and epithelial cells (34) and *in vitro* experiments with prostate cancer cell lines have shown a marked increase in HDAC levels for most HDACs compared with normal prostate tissue (35). Although it is thought that acetylation of histones is required for gene expression, inhibiting HDACs does not result in whole-genome reexpression. In fact, about half of the genes that are differentially expressed after VPA treatment are down-regulated (36).

Nuclear organization and chromatin dynamics have regained interest because recent reports suggest that, in interphase cells, gene activation and replication is associated with repositioning of the genetic locus relative to the nuclear compartment and other genomic loci (37, 38). Although individual chromosomes occupy distinct positions in the nucleus called chromosome territories (39), locus-specific movement within and across these boundaries occurs throughout the interphase. The (extent of) mobility of individual loci depends on nuclear localization (40), phase in cell cycle (41), and location on the chromosome (42) and might be actin-, myosin-, and ATP-dependent (43, 44). Although in many cases repositioning of activated genes is oriented toward the nuclear interior (44–48), there is not always a strict correlation between movement away from the periphery and gene activation (4647, 49). The purpose of these movements and the means by which this is possible is under intense debate. It is suggested that chromatin

mobility may facilitate access for enzymes involved in histone modifications, nucleosome remodeling, and the ensuing folding or unfolding of the domain (38). Recently, investigators have described the existence of regulatory cross-talk between "kissing" loci within and across chromosomes, suggesting the existence of spatial networks of gene regulation. They propose that interacting loci form a "poised chromatin hub," which might recruit remodeling complexes or histone acetyltransferases to form a positive environment for gene expression (50, 51). As described above, it is known that chromatin remodeling proteins such as high-mobility group proteins and the SWI/SNF complex are (in part) regulated by acetylation. Furthermore, it has been shown that acetylation is deregulated in cancer cells (2, 3).

In the current study, we show that VPA treatment results in dose- and time-dependent changes in the nuclear structure of prostate cancer cell lines, reflecting change in chromatin remodeling dynamics in prostate cancer cells. Further, these nuclear morphometric alterations can be used as a marker to measure therapeutic response. With the automated CoolScope, results can be easily calibrated and laboratory-dependent variation can be minimized. Of note, VPA treatment also induces nuclear structural changes in the mouse normal liver and kidney cells where it is metabolized and its breakdown products are excreted (52). These nuclear structural changes in normal liver and kidney cells may reflect underlying cause for reported elevation of liver enzyme, hepatitis, renal tubular dysfunction in children (53), and Fanconi syndrome (54, 55) during VPA treatment.

Previously, our group has shown that VPA treatment of prostate cancer cells increases histone H3 acetylation, CK18, and p21 and p27 expression and decreases androgen receptor, cyclin D1, and Ki-67 expression *in vitro* and *in vivo* (56, 57). Further, chronic low-dose administration of VPA results in an increase in apoptosis (assessed by TUNEL assay) and a decrease in angiogenesis (assessed by CD34 microvessel density) in prostate cancer xenografts (56). The next step in our investigation, the analysis of pretreatment and posttreatment human prostate cancer tissue, is not feasible for now, as VPA treatment for solid tumors is only given in a clinical trial setting at the moment. Patients eligible for a clinical trial are in an end stage of their disease and typically have had a prostatectomy or chemotherapy before enrollment.

Supplementary Tables S1[4] and S2[4] illustrate that *in vitro* and *in vivo* prostate cancer-treated cells had different structural alterations profiles. There are several potential reasons that may explain these differences. Chromatin remodeling and actin filament organization are interacting processes (58). It is known that the nucleus forms part of a continuous physical network spanning the extracellular matrix, the cytoskeleton, and the nuclear envelope. Environmentally mediated forces can be transmitted to the nucleus and induce deformations of the chromatin (59). In our experiments, *in vitro* cells were grown in a single layer in a dish before harvesting using trypsin, whereas *in vivo* cells were grown three-dimensionally in mouse stroma and were paraffin-embedded as such. In addition, *in vitro* and *in vivo* cells have access to a different set of growth factors and other nutrients. Their microenvironment differs grossly, which might affect their type of response to VPA treatment.

The quantitative assessment of nuclear structure by digital image analysis has identified numerous potential clinical applications. Our group has previously shown that there are significant alterations in nuclear structure between and within Gleason grading patterns 3 to 5 (60). Further, we showed that nuclear structure analysis is of additive value

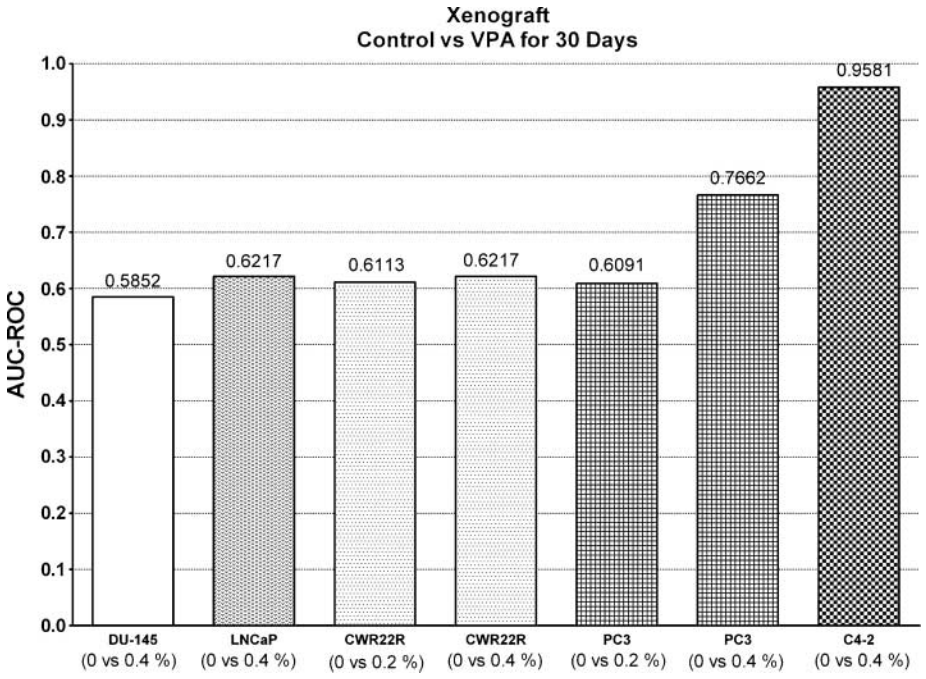

Figure 3. Summary of AUC-ROC statistics of control versus *in vivo* treated cell lines. Response (AUC-ROC) of DU145, LNCaP, CWR22R, PC3, and C4-2 cell lines treated *in vivo* with different doses (0, 0.2%, and 0.4%) VPA in drinking water for 30 d.

with clinicopathologic parameters in the prediction of biochemical recurrence, distant metastasis, and death after radical prostatectomy (23, 24). Recently, Makarov et al. (61) used quantitative nuclear structure alterations to predict conversion to unfavorable biopsy pathology during watchful waiting surveillance. In this article, we discuss the use of nuclear structure analysis in therapeutic response measurements. Identification of proteins that modify nuclear chromatin organization is of paramount importance to improve our understanding of the biology behind these measurements. One of such proteins was histone acetyltransferase protein p300 has shown to predict prostate cancer biochemical recurrence in men with long-term follow-up and correlate with changes in epithelia nuclear size and shape (62–64). The use of quantitative nuclear structure alterations and the molecular mechanisms that cause such changes provide the foundation for continued research in this area that can eventually change the management of prostate cancer patients.

In conclusion, HDACI VPA significantly changes the epithelial nuclear structure in a time- and dose-dependent fashion in prostate cancer both *in vitro* and *in vivo*. VPA also affects nuclear structure in normal mouse liver and kidney tissue, which likely reflects a natural physiologic response.

Disclosure of Potential Conflicts of Interest

No potential conflicts of interest were disclosed.

Acknowledgments

We thank Shabana Shabbeer for providing xenograft material.

References

1. Kortenhorst MS, Carducci MA, Shabbeer S. Acetylation and histone deacetylase inhibitors in cancer. Cell Oncol 2006;28:191–222.

2. Johnstone RW. Histone-deacetylase inhibitors: novel drugs for the treatment of cancer. Nat Rev Drug Discov 2002;1:287–99.

3. Weichert W, Roske A, Gekeler V, et al. Association of patterns of class I histone deacetylase expression with patient prognosis in gastric cancer: a retrospective analysis. Lancet Oncol 2008;9:139–48.

4. Reid T, Valone F, Lipera W, et al. Phase II trial of the histone deacetylase inhibitor pivaloyloxymethyl butyrate (Pivanex, AN-9) in advanced non-small cell lung cancer. Lung Cancer 2004;45:381–6.

5. Kelly WK, O'Connor OA, Krug LM, et al. Phase I study of an oral histone deacetylase inhibitor, suberoylanilide hydroxamic acid, in patients with advanced cancer. J Clin Oncol 2005;23:3923–31.

6. Atmaca A, Al-Batran SE, Maurer A, et al. Valproic acid (VPA) in patients with refractory advanced cancer: a dose escalating phase I clinical trial. Br J Cancer 2007;97:177–82.

7. Soriano AO, Yang H, Faderl S, et al. Safety and clinical activity of the combination of 5-azacytidine, valproic acid, and all-trans retinoic acid in acute myeloid leukemia and myelodysplastic syndrome. Blood 2007; 110:2302–8.

8. Kim B, Ahn K, Kim I, Park I, Kim B, Yoon S. Effect of combined treatment of bortezomib and valproic acid on multiple myeloma cells. ASCO Annu Meet Proc Part I 2007;18539.

9. Braiteh F, Soriano AO, Garcia-Manero G, et al. Phase I study of epigenetic modulation with 5-azacytidine and valproic acid in patients with advanced cancers. Clin Cancer Res 2008;14:6296–301.

10. Munster P, Marchion D, Bicaku E, et al. Phase I trial of histone deacetylase inhibition by valproic acid followed by the topoisomerase II inhibitor epirubicin in advanced solid tumors: a clinical and translational study. J Clin Oncol 2007;25:1979–85.

11. Waterborg JH. Dynamics of histone acetylation *in vivo*. A function for acetylation turnover? Biochem Cell Biol 2002;80:363–78.

12. Escargueil AE, Soares DG, Salvador M, Larsen AK, Henriques JA. What histone code for DNA repair? Mutat Res 2008;658:259–70.

13. Polevoda B, Sherman F. The diversity of acetylated proteins. Genome Biol 2002;3:reviews0006.

14. Ferguson M, Henry PA, Currie RA. Histone deacetylase inhibition is associated with transcriptional repression of the Hmga2 gene. Nucleic Acids Res 2003;31:3123–33.

15. Zhang Q, Wang Y. High mobility group proteins and their post-translational modifications. Biochim Biophys Acta 2008;1784:1159–66.

16. Lim JH, West KL, Rubinstein Y, Bergel M, Postnikov YV, Bustin M. Chromosomal protein HMGN1 enhances the acetylation of lysine 14 in histone H3. EMBO J 2005;24:3038–48.

17. Belova GI, Postnikov YV, Furusawa T, Birger Y, Bustin M. Chromosomal protein HMGN1 enhances the heat shock-induced remodeling of Hsp70 chromatin. J Biol Chem 2008;283:8080–8.

18. Townson SM, Kang K, Lee AV, Oesterreich S. Structure-function analysis of the estrogen receptor α corepressor scaffold attachment factor-B1: identification of a potent transcriptional repression domain. J Biol Chem 2004;279:26074–81.

19. MacRae TH. Tubulin post-translational modifications—enzymes and their mechanisms of action. Eur J Biochem 1997;244:265–78.

20. Haggarty SJ, Koeller KM, Wong JC, Grozinger CM, Schreiber SL. Domain-selective small-molecule inhibitor of histone deacetylase 6 (HDAC6)-mediated tubulin deacetylation. Proc Natl Acad Sci U S A 2003;100: 4389–94.

21. Yamamichi N, Yamamichi-Nishina M, Mizutani T, et al. The Brm gene suppressed at the post-transcriptional level in various human cell lines is inducible by transient HDAC inhibitor treatment, which exhibits antioncogenic potential. Oncogene 2005;24:5471–81.

22. Diamond DA, Berry SJ, Jewett HJ, Eggleston JC, Coffey DS. A new method to assess metastatic potential of human prostate cancer: relative nuclear roundness. J Urol 1982;128:729–34.

23. Veltri RW, Miller MC, Isharwal S, Marlow C, Makarov DV, Partin AW. Prediction of prostate-specific antigen recurrence in men with long-term follow-up postprostatectomy using quantitative nuclear morphometry. Cancer Epidemiol Biomarkers Prev 2008;17:102–10.

24. Veltri RW, Khan MA, Miller MC, et al. Ability to predict metastasis based on pathology findings and alterations in nuclear structure of normal-appearing and cancer peripheral zone epithelium in the prostate. Clin Cancer Res 2004;10:3465–73.

25. Partin AW, Walsh AC, Pitcock RV, Mohler JL, Epstein JI, Coffey DS. A comparison of nuclear morphometry and Gleason grade as a predictor of prognosis in stage A2 prostate cancer: a critical analysis. J Urol 1989; 142:1254–8.

26. Epstein JI, Berry SJ, Eggleston JC. Nuclear roundness factor. A predictor of progression in untreated stage A2 prostate cancer. Cancer 1984; 54:1666–71.

27. Huisman A, Ploeger LS, Dullens HF, et al. Discrimination between benign and malignant prostate tissue using chromatin texture analysis in 3-D by confocal laser scanning microscopy. Prostate 2007;67:248–54.

28. Jorgensen T, Yogesan K, Tveter KJ, Skjorten F, Danielsen HE. Nuclear texture analysis: a new prognostic tool in metastatic prostate cancer. Cytometry 1996;24:277–83.

29. Stein GS, Lian JB, Stein JL, et al. Combinatorial organization of the transcriptional regulatory machinery in biological control and cancer. Adv Enzyme Regul 2005;45:136–54.

30. Carmichael MJ, Veltri RW, Partin AW, Miller MC, Walsh PC, Epstein JI. Deoxyribonucleic acid ploidy analysis as a predictor of recurrence following radical prostatectomy for stage T_2 disease. J Urol 1995;153:1015–9.

31. Gill JE, Jotz MM. Further observations on the chemistry of pararosaniline-Feulgen staining. Histochemistry 1976;46:147–60.

32. Schulte E, Wittekind D. Standardization of the Feulgen-Schiff technique. Staining characteristics of pure fuchsin dyes; a cytophotometric investigation. Histochemistry 1989;91:321–31.

33. Grignani F, De Matteis S, Nervi C, et al. Fusion proteins of the retinoic acid receptor-α recruit histone deacetylase in promyelocytic leukaemia. Nature 1998;391:815–8.

34. Waltregny D, North B, Van Mellaert F, de Leval J, Verdin E, Castronovo V. Screening of histone deacetylases (HDAC) expression in human prostate

cancer reveals distinct class I HDAC profiles between epithelial and stromal cells. Eur J Histochem 2004;48:273–90.

35. Kachhap SK, Kortenhorst MSQ, Shabbeer S, Washington E, Carducci MA. Comparison of expression of class I and class II histone deacetylase in prostate cancer cell lines and normal immortalized prostate epithelial cells. Proc AACR Annu Meet 2005;46:648 (abstr 2751).

36. Kortenhorst MS, Zahurak M, Shabbeer S, et al. A multiple-loop, double-cube microarray design applied to prostate cancer cell lines with variable sensitivity to histone deacetylase inhibitors. Clin Cancer Res 2008;14:6886–94.

37. Lanctot C, Cheutin T, Cremer M, Cavalli G, Cremer T. Dynamic genome architecture in the nuclear space: regulation of gene expression in three dimensions. Nat Rev Genet 2007;8:104–15.

38. Gasser SM. Visualizing chromatin dynamics in interphase nuclei. Science 2002;296:1412–6.

39. Cremer T, Cremer M, Dietzel S, Muller S, Solovei I, Fakan S. Chromosome territories—a functional nuclear landscape. Curr Opin Cell Biol 2006; 18:307–16.

40. Chubb JR, Boyle S, Perry P, Bickmore WA. Chromatin motion is constrained by association with nuclear compartments in human cells. Curr Biol 2002;12:439–45.

41. Thomson I, Gilchrist S, Bickmore WA, Chubb JR. The radial positioning of chromatin is not inherited through mitosis but is established *de novo* in early G_1. Curr Biol 2004;14:166–72.

42. Heun P, Laroche T, Shimada K, Furrer P, Gasser SM. Chromosome dynamics in the yeast interphase nucleus. Science 2001;294:2181–6.

43. Levi V, Ruan Q, Plutz M, Belmont AS, Gratton E. Chromatin dynamics in interphase cells revealed by tracking in a two-photon excitation microscope. Biophys J 2005;89:4275–85.

44. Chuang CH, Carpenter AE, Fuchsova B, Johnson T, de Lanerolle P, Belmont AS. Long-range directional movement of an interphase chromosome site. Curr Biol 2006;16:825–31.

45. Kosak ST, Skok JA, Medina KL, et al. Subnuclear compartmentalization of immunoglobulin loci during lymphocyte development. Science 2002;296:158–62.

46. Hewitt SL, High FA, Reiner SL, Fisher AG, Merkenschlager M. Nuclear repositioning marks the selective exclusion of lineage-inappropriate transcription factor loci during T helper cell differentiation. Eur J Immunol 2004;34:3604–13.

47. Williams RR, Azuara V, Perry P, et al. Neural induction promotes large-scale chromatin reorganisation of the Mash1 locus. J Cell Sci 2006;119: 132–40.

48. Zink D, Amaral MD, Englmann A, et al. Transcription-dependent spatial arrangements of CFTR and adjacent genes in human cell nuclei. J Cell Biol 2004;166:815–25.

49. Ragoczy T, Bender MA, Telling A, Byron R, Groudine M. The locus control region is required for association of the murine β-globin locus with engaged transcription factories during erythroid maturation. Genes Dev 2006;20:1447–57.

50. Spilianakis CG, Lalioti MD, Town T, Lee GR, Flavell RA. Interchromosomal associations between alternatively expressed loci. Nature 2005; 435:637–45.

51. Simonis M, Klous P, Splinter E, et al. Nuclear organization of active and inactive chromatin domains uncovered by chromosome conformation capture-on-chip (4C). Nat Genet 2006;38:1348–54.

52. Gilman AG, Rall TW, Nies AS, Taylor P. Goodman and Gilman's the pharmacological basis of therapeutics. Goodman and Gilman's the pharmacological basis of therapeutics. 8th ed. New York: Pergamon Press; 1990 pp. 450–3.

53. Altunbasak S, Yildizas D, Anarat A, Burgut HR. Renal tubular dysfunction in epileptic children on valproic acid therapy. Pediatr Nephrol 2001; 16:256–9.

54. Watanabe T, Yoshikawa H, Yamazaki S, Abe Y, Abe T. Secondary renal Fanconi syndrome caused by valproate therapy. Pediatr Nephrol 2005; 20:814–7.

55. Knorr M, Schaper J, Harjes M, Mayatepek E, Rosenbaum T. Fanconi syndrome caused by antiepileptic therapy with valproic acid. Epilepsia 2004;45:868–71.

56. Shabbeer S, Kortenhorst MS, Kachhap S, Galloway N, Rodriguez R, Carducci MA. Multiple molecular pathways explain the anti-proliferative effect of valproic acid on prostate cancer cells *in vitro* and *in vivo*. Prostate 2007;67:1099–110.

57. Xia Q, Sung J, Chowdhury W, et al. Chronic administration of valproic acid inhibits prostate cancer cell growth *in vitro* and *in vivo*. Cancer Res 2006;66:7237–44.

58. Farrants AK. Chromatin remodelling and actin organisation. FEBS Lett 2008;582:2041–50.

59. Verstraeten VL, Lammerding J. Experimental techniques for study of chromatin mechanics in intact nuclei and living cells. Chromosome Res 2008;16:499–510.

60. Veltri RW, Marlow C, Khan MA, Miller MC, Epstein JI, Partin AW. Significant variations in nuclear structure occur between and within Gleason grading patterns 3, 4, and 5 determined by digital image analysis. Prostate 2007;67:1202–10.

61. Makarov DV, Marlow C, Epstein JI, et al. Using nuclear morphometry to predict the need for treatment among men with low grade, low stage prostate cancer enrolled in a program of expectant management with curative intent. Prostate 2008;68:183–9.

62. Isharwal S, Miller MC, Marlow C, Makarov DV, Partin AW, Veltri RW. p300 (histone acetyltransferase) biomarker predicts prostate cancer biochemical recurrence and correlates with changes in epithelia nuclear size and shape. Prostate 2008;68:1097–104.

63. Debes JD, Sebo TJ, Heemers HV, et al. p300 modulates nuclear morphology in prostate cancer. Cancer Res 2005;65:708–12.

64. Debes JD, Sebo TJ, Lohse CM, Murphy LM, Haugen DA, Tindall DJ. p300 in prostate cancer proliferation and progression. Cancer Res 2003; 63:7638–40.